Computation of Complex Resonance Frequencies of Isolated Composite Objects

WENXIN ZHENG

Abstract—A technique based on the null-field method is developed to investigate the resonance frequencies and the quality factors of isolated composite dielectric/ferrite resonators. A method of identifying the resonant modes is suggested for nonspherical resonators by analyzing the peaks of their scattering cross sections in the resonance frequency range. Computed resonance frequencies and Q factors for composite resonators, such as double disks and tubular resonators with ferrite core, are compared with published calculations and experiments whenever possible. These comparisons show that the present technique is an effective and flexible one for investigating composite resonators with relatively complicated geometries.

I. Introduction

DIELECTRIC resonators for applications in microwave and millimeter-wave systems have received increasing attention during the past decade. Many analytic and numerical methods have been developed for the analysis of such resonators. For example, there are the perfect magnetic conducting wall (PMC) methods [1] and the dielectric waveguide methods [2] as well as their perturbational corrections and variational improvements [3] for cylindric resonators; various radial and axial mode matching methods [4]–[6] for shielded resonators; the asymptotic expansion methods [7], [8] for resonators with very high permittivities; the moment method based on the surface integral techniques [9], [10] for isolated resonators; and the general mode-matching approaches using Green's dyadic functions or transverse modes in expanding the interior and exterior fields for shielded or open homogeneous resonators [11], [12]. The merits and shortcomings of most of these methods are described and compared in [3] and [11].

In the present article, we utilize the null-field method, which is also called the T-matrix method or the extended boundary condition method, for the investigation of inhomogeneous dielectric and ferrite resonators with star-shaped geometries and structures (for example, pillboxes, rings, double disks, and superellipsoids) for any azimuthal variation (including hybrid modes with $m \neq 0$). The method can be used to analyze both isolated and metallic shielded resonators. In this paper, we shall concentrate our attention on isolated resonators (permeable resonators in free space). The null-field method was mainly developed for scattering problems from both homogeneous [13], [14] and composite scatterers [15], [16]. It has also been employed to investigate passbands of electromagnetic waveguides [17], [18], resonance scattering of homogeneous dielectric objects [19], and natural frequencies of conducting disks [20]. A formulation for transient fields was given in [21] and [22]. This formulation provides in particular an alternative way of finding the complex resonance frequencies. However, in the present work we base our computations on the time-harmonic null-field approach. An excellent review of complex frequency computations in this framework is given in [20]. Extensive computations of complex resonance frequencies using this approach have been performed for perfectly reflecting objects in acoustics, electromagnetics, and elastodynamics and for dielectrically coated spheres (see, e.g., [23], [24] and references given therein). In [25], the time-harmonic null-field approach was used to find complex resonance frequencies of a dielectric resonator.

The main procedure of the null-field approach to resonance problems can be summarized as follows. The surface fields (electric and magnetic currents) on all surfaces and interfaces between homogeneous parts of a composite body, which are excited by an incident field, are approximated in terms of global expansion functions with as-yet-unknown coefficients. By applying the null part of Green's second theorem to every homogeneous region of the resonator and introducing those expansions of surface fields and the boundary conditions, an infinite homogeneous system of simultaneous linear equations is obtained for the expansion coefficients under zero excitation. This system has nontrivial solutions only when its determinant vanishes. Hence, the resonance frequencies can be found by searching for the zeros of the determinant. In practice, the system is truncated to a finite size and computations are repeated with increasing truncation orders until a specific convergence requirement is met.

A brief review of a null-field approach derived in [26], which is suitable for analysis of an isolated composite dielectric and/or ferrite resonator, is given in Section II.

Manuscript received August 30, 1988; revised January 20, 1989.

The author is with the Department of Electromagnetic Theory, Royal Institute of Technology, S-100 44 Stockholm, Sweden.

IEEE Log Number 8927160.

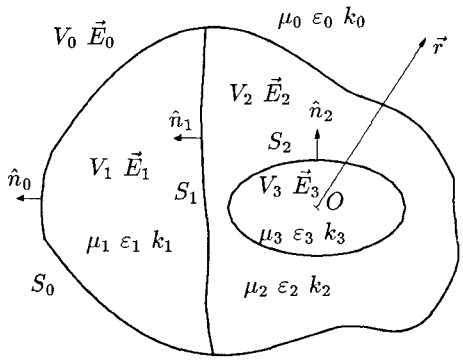

Fig. 1. Geometry and notations of a composite resonator consisting of three homogeneous parts.

In principle, the method described in Section II is applicable for general three-dimensional star-shaped resonators. In Section III we discuss the classification of TE, TM, and HEM modes and compare our results with published data for axisymmetric resonators of the kind encountered in actual microwave circuits. Results of composite resonators are given in Section IV, in particular for a type of frequency tunable resonator that consists of a dielectric ring and a ferrite core. Section V gives some general concluding remarks.

II. Formulations

We consider the general case of a resonator which consists of N homogeneous parts (an example with three homogeneous parts is given in Fig. 1). We assume that it has a star-shaped core, occupying the volume V_N, and $N-1$ parts which are not required to be star-shaped occupying the volumes V_i, $i=1,2,\cdots,N-1$. An object is said to be star-shaped if one can find an interior point such that the magnitude $r(\theta,\phi)$ of the radius vector $\vec{r}$ from this point to any point on the surface of the object is a single-valued function of the spherical angles θ and ϕ. Hence, a fixed origin O can be chosen inside V_N and vector spherical waves or vector spherical harmonics defined with respect to this origin can be used to approximate the surface fields. The composite resonator is now assumed to have the geometric property that if one removes the homogeneous parts one by one, starting from V_1 and ending at V_{N-1} in the order of increasing index, then at each step the exterior bounding surface of the remaining object is star shaped as seen from the origin O. As an example, the three-part resonator shown in Fig. 1 satisfies this requirement. In the following we also assume that the exterior region V_0 is filled with homogeneous material and that the electromagnetic properties of the homogeneous material in every region V_i, $i=0,1,\cdots,N$, can be described by a scalar relative permittivity ϵ_i and a scalar relative permeability μ_i. Then the wavenumber k_i in V_i can be expressed in terms of a signal frequency, ν, as $k_i = k_0\sqrt{\epsilon_i\mu_i} = 2\pi\nu\sqrt{\epsilon_i\mu_i}/c$, where c is the speed of light in vacuum.

We denote the bounding surface of the volume $\sum_{j=i+1}^{N} V_j$ by S_i, $i=0,1,\cdots,N-1$, and the outward unit normal on S_i by $\hat{n}_i$. Taking the object in Fig. 1 as an example, we find that S_0 is the enclosing surface of the whole object, S_1 the exterior surface of V_2, and S_2 the interface between V_2 and V_3. We note that all of the surfaces S_i, $i=0,1,\cdots,N-1$, are closed and that the adjacent surfaces S_{i-1} and S_i may overlap in some area as S_0 and S_1 do on the right side of the object in Fig. 1, but they never intersect (cross) one another. Furthermore, we assume that there is a thin layer inside the common part of S_{i-1} and S_i, if there is any common part at all, having material properties ϵ_i and μ_i. Then we obtain a fictitious layered object where each annular region V_i, $i=1,2,\cdots,N-1$, is bounded externally by S_{i-1} and internally by S_i. The electric field in the annular region V_i is denoted by $\vec{E}_i$. It has been shown in [26] that it is feasible to first derive formulations considering the layered structure, and then compute results for the real composite object by setting the thickness equal to zero for all the fictitious layers inside the common parts of the surfaces. Various null-field approaches to scattering from layered scatterers are derived and discussed in [26]–[28]. In the present article we make use of the general formulation given in [26, sec. IV]. Numerical experiments suggest that in general this is the most suitable one for the open dielectric and ferrite resonators considered here.

Suppose that an object is excited by a known incident field $\vec{E}^{\text{in}}$. The total field in the exterior region can be expressed as the sum of the incident field $\vec{E}^{\text{in}}$ and the unknown scattered field $\vec{E}^{\text{sc}}$: $\vec{E}_0(\vec{r}) = \vec{E}^{\text{in}}(\vec{r}) + \vec{E}^{\text{sc}}(\vec{r})$. As is well known, the incident and scattered fields can be expanded in terms of regular and outgoing spherical waves, respectively (see, e.g., [27]):

$$\vec{E}^{\text{in}}(\vec{r}) = \sum_n a_n Re\vec{\psi}_n(k_0\vec{r}) \tag{1}$$

$$\vec{E}^{\text{sc}}(\vec{r}) = \sum_n f_n\vec{\psi}_n(k_0\vec{r}). \tag{2}$$

The outgoing spherical waves are defined as

$$\begin{aligned}\vec{\psi}_n(k\vec{r}) &\equiv \vec{\psi}_{\tau\sigma ml}(k\vec{r}) \equiv \vec{\psi}_\tau\begin{pmatrix} e \\ o \end{pmatrix}_{ml}(k\vec{r}) \equiv \\ &\equiv \gamma_{ml}^{1/2}(k^{-1}\nabla\times)^\tau \\ &\quad\cdot\left[k\vec{r}P_l^m(\cos\theta)\begin{pmatrix}\cos m\phi \\ \sin m\phi\end{pmatrix}h_l^{(1)}(kr)\right]\end{aligned} \tag{3}$$

where

$$\begin{aligned}&\tau = 1,2 \qquad \sigma = e, o\ (\text{"even" or "odd"}) \\ &m = 0,1,\cdots,l \qquad l = 1,2,\cdots \\ &\gamma_{ml} = \frac{(2-\delta_{m0})(2l+1)(l-m)!}{4\pi l(l+1)(l+m)!}.\end{aligned}$$

The regular wave $Re\vec{\psi}_n(k\vec{r})$ is defined in an analogous way with the spherical Hankel function $h_l^{(1)}(kr)$ replaced by the spherical Bessel function $j_l(kr)$. An abbreviated notation using the multi-index $n \equiv (\tau,\sigma,m,l)$ has been used. The time factor is $e^{-i\omega t}$. The expansion (1) is valid inside any sphere with center at O which does not contain any of the sources of $\vec{E}^{\text{in}}$. The expansion (2) is valid outside any sphere with center at O which encloses the exterior surface of the resonator. An implicit relation between $\{f_n\}$ and $\{a_n\}$ is obtained from Green's second

theorem applied to the region V_0 [13]. The null part gives (the "null-field equations"):

$$a_n = -ik_0\int_{S_0}\left[\nabla'\times\vec{\psi}_n(k_0\vec{r}')\cdot(\hat{n}_0\times\vec{E}_0) + \vec{\psi}_n(k_0\vec{r}')\cdot(\hat{n}_0\times(\nabla'\times\vec{E}_0))\right]dS' \quad (4)$$

and the remaining part of the theorem gives

$$f_n = ik_0\int_{S_0}\left[\nabla'\times Re\vec{\psi}_n(k_0\vec{r}')\cdot(\hat{n}_0\times\vec{E}_0) + Re\vec{\psi}_n(k_0\vec{r}')\cdot(\hat{n}_0\times(\nabla'\times\vec{E}_0))\right]dS'. \quad (5)$$

In order to obtain matrix relations between $\{f_n\}$, $\{a_n\}$ and the surface fields $\hat{n}\times\vec{E}_0$ and $\hat{n}\times(\nabla\times\vec{E}_0)$, we need to take into account the boundary conditions on all interfaces. By considering the resonator as a limit of a "layered" object, one can write the boundary condition as

$$\hat{n}_i\times\vec{E}_i(\vec{r}') = \hat{n}_i\times\vec{E}_{i+1}(\vec{r}') \quad (6)$$

$$(1/\mu_i)\hat{n}_i\times(\nabla'\times\vec{E}_i(\vec{r}')) = (1/\mu_{i+1})\hat{n}_i\times(\nabla'\times\vec{E}_{i+1}(\vec{r}')) \quad (7)$$

$$\vec{r}' \text{ on } S_i; \qquad i=0,1,\cdots,N-1.$$

The expansions of the surface fields are written as

$$\hat{n}_{i-1}\times\vec{E}_i(\vec{r}) = \sum_{n'}\alpha_{n'}^{(i)}\left[\hat{n}_{i-1}\times\vec{\Phi}'_{n'}\right]$$

$$\hat{n}_{i-1}\times(\nabla\times\vec{E}_i(\vec{r})) = \sum_{n'}\beta_{n'}^{(i)}\left[\hat{n}_{i-1}\times\vec{\Phi}''_{n'}\right] \quad (8)$$

$$i=1,2,\cdots,N$$

on the inside of S_{i-1}. In these expansions, $\{\vec{\Phi}'_n\}$ and $\{\vec{\Phi}''_n\}$ are two arbitrary sets of global functions which are complete on the corresponding surface (these sets may be identical to each other). As discussed in [14] and [26], many types of expansions are available for (8). In the present article we shall only use the sets

$$\vec{\Phi}'_n \equiv Re\vec{\psi}_n(k_N\vec{r}) \quad (9)$$

$$\vec{\Phi}''_n \equiv \nabla\times Re\vec{\psi}_n(k_N\vec{r}) \quad (10)$$

on the surface of the core, S_{N-1}, which means that we obtain $\alpha_n^{(N)} = \beta_n^{(N)}$ (cf., e.g., [14]), and

$$\vec{\Phi}'_n \equiv \vec{\Phi}''_n \equiv \vec{A}_n \quad (11)$$

on the outer surfaces S_i, $i=0,1,\cdots,N-2$, where $\vec{A}_n$ denotes the vector spherical harmonics. The explicit form of $\vec{A}_n$ is

$$\vec{A}_n \equiv \begin{cases} \vec{A}_1\binom{e}{o}_{ml}(\hat{r}) \equiv \gamma_{ml}^{1/2}\nabla\times\left[\vec{r}P_l^m(\cos\theta)\begin{pmatrix}\cos m\phi\\ \sin m\phi\end{pmatrix}\right] \\ \vec{A}_2\binom{e}{o}_{ml}(\hat{r}) \equiv \gamma_{ml}^{1/2}r\nabla\left[P_l^m(\cos\theta)\begin{pmatrix}\cos m\phi\\ \sin m\phi\end{pmatrix}\right] \end{cases} \quad (12)$$

where the multi-index n and the normalization factor γ_{ml} are the same as in (3). Our numerical experience indicates that the choice given by (11) is generally the most useful one.

Equations (6)–(8) are now introduced into (4) and (5) and with the use of a vector and matrix notation ($\vec{a}\equiv\{a_n\}$, $\boldsymbol{Q}\equiv\{Q_{nn'}\}$, etc.), we obtain

$$\vec{a} = i\left[\boldsymbol{Q}_A^{S_0}(\vec{\psi}_0,\vec{\Phi}')\vec{\alpha}^{(1)} + \boldsymbol{Q}_B^{S_0}(\vec{\psi}_0,\vec{\Phi}'')\vec{\beta}^{(1)}\right] \quad (13)$$

$$\vec{f} = -i\left[\boldsymbol{Q}_A^{S_0}(Re\vec{\psi}_0,\vec{\Phi}')\vec{\alpha}^{(1)} + \boldsymbol{Q}_B^{S_0}(Re\vec{\psi}_0,\vec{\Phi}'')\vec{\beta}^{(1)}\right] \quad (14)$$

where elements of the Q matrices are defined by

$$\left[\boldsymbol{Q}_A^{S_i}(\vec{\Psi}_p,\vec{\Phi})\right]_{nn'} = k_p\int_{S_i}\left[\nabla'\times\vec{\Psi}_n(k_p\vec{r}')\right]\times\vec{\Phi}_{n'}\cdot\hat{n}_i\,dS'$$

$$\left[\boldsymbol{Q}_B^{S_i}(\vec{\Psi}_p,\vec{\Phi})\right]_{nn'} = k_p\int_{S_i}\frac{\mu_p}{\mu_{p+1}}\left[\vec{\Psi}_n(k_p\vec{r}')\cdot\vec{\Phi}_{n'}\right]\cdot\hat{n}_i\,dS' \quad (15)$$

$$\boldsymbol{Q}^{S_i}(\vec{\Psi}_p,\vec{\Phi}) = \boldsymbol{Q}_A^{S_i}(\vec{\Psi}_p,\vec{\Phi}) + \boldsymbol{Q}_B^{S_i}(\vec{\Psi}_p,\nabla\times\vec{\Phi}).$$

Applying Green's theorem to the "annular" region V_i, $i=1,2,\cdots,N-1$, step by step, and introducing boundary conditions and corresponding expansions, we get the following relations between the coefficients of the surface fields:

$$\boldsymbol{Q}_A^{S_{i-1}}(Re\vec{\psi}_i,\vec{\Phi}')\vec{\alpha}^{(i)} + \boldsymbol{Q}_B^{S_{i-1}}(Re\vec{\psi}_i,\vec{\Phi}'')\vec{\beta}^{(i)} = \boldsymbol{Q}_A^{S_i}(Re\vec{\psi}_i,\vec{\Phi}')\vec{\alpha}^{(i+1)} + \boldsymbol{Q}_B^{S_i}(Re\vec{\psi}_i,\vec{\Phi}'')\vec{\beta}^{(i+1)} \quad (16)$$

$$\boldsymbol{Q}_A^{S_{i-1}}(\vec{\psi}_i,\vec{\Phi}')\vec{\alpha}^{(i)} + \boldsymbol{Q}_B^{S_{i-1}}(\vec{\psi}_i,\vec{\Phi}'')\vec{\beta}^{(i)} = \boldsymbol{Q}_A^{S_i}(\vec{\psi}_i,\vec{\Phi}')\vec{\alpha}^{(i+1)} + \boldsymbol{Q}_B^{S_i}(\vec{\psi}_i,\vec{\Phi}'')\vec{\beta}^{(i+1)} \quad (17)$$

$$\text{for } i=1,2,\cdots,N-1.$$

The elimination of the surface field coefficients in (13)–(17) can be done in such a way that $\vec{\alpha}^{(i)}, \vec{\beta}^{(i)}$, $i=1,\cdots,N-1$, are expressed in terms of $\vec{\alpha}^{(N)}$. We define

$$Q(i,j) \equiv \begin{pmatrix} \boldsymbol{Q}_A^{S_i}(Re\vec{\psi}_j,\vec{\Phi}'), & \boldsymbol{Q}_B^{S_i}(Re\vec{\psi}_j,\vec{\Phi}'') \\ \boldsymbol{Q}_A^{S_i}(\vec{\psi}_j,\vec{\Phi}'), & \boldsymbol{Q}_B^{S_i}(\vec{\psi}_j,\vec{\Phi}'') \end{pmatrix}. \quad (18)$$

If the result of the above-mentioned scheme is introduced into (13) and (14), the latter can be written as

$$\vec{a} = i\boldsymbol{Q}(N,\vec{\psi})\vec{\alpha}^{(N)} \quad (19)$$

$$\vec{f} = -i\boldsymbol{Q}(N,Re\vec{\psi})\vec{\alpha}^{(N)} \quad (20)$$

where

$$\begin{pmatrix}\boldsymbol{Q}(N,Re\vec{\psi})\\ \boldsymbol{Q}(N,\vec{\psi})\end{pmatrix} \equiv Q(0,0)\cdot Q^{-1}(0,1)\cdot Q(1,1)\cdot\cdots Q(i,i)\cdot Q^{-1}(i,i+1)\cdot\cdots Q(N-2,N-2)\cdot Q^{-1}(N-2,N-1)\cdot\begin{pmatrix}\boldsymbol{Q}^{S_{N-1}}(Re\vec{\psi}_{N-1},Re\vec{\psi}(k_N\vec{r}))\\ \boldsymbol{Q}^{S_{N-1}}(\vec{\psi}_{N-1},Re\vec{\psi}(k_N\vec{r}))\end{pmatrix}. \quad (21)$$

The scattered field of an object is the solution of an inhomogeneous wave equation under the excitation of an incident field, while the resonant field of the object is the eigensolution of the corresponding homogeneous equation (without any excitation). This means that the scattered field $\vec{E}^{sc}$ can be obtained from (1), (2), (19), and (20) if there is a known incident wave $\vec{E}^{in}$ (i.e., $\vec{a}$ is known), and that the resonant fields can also be computed from the

same equations by setting $\vec{a}=0$. In order to have nontrivial solutions of (20), i.e., resonant fields of various resonant modes, when $\vec{a}=0$, the determinant of $\boldsymbol{Q}(N,\vec{\psi})$ in (19) must be zero:

$$\det\left[\boldsymbol{Q}\left(N,\vec{\psi}\right)\right]=0. \tag{22}$$

From (21), (18), and (15) we see that the elements of the matrix $\boldsymbol{Q}(N,\vec{\psi})$ depend upon the geometry and the material properties of a resonator as well as the wavenumber k_0. For a given resonator, one can compute the resonance frequencies by searching for k_0's which satisfy (22). Suppose that the value k_{0_i} $(i=1,2,\cdots)$ is the ith root of (22); the resonance frequencies ν_i of the resonator can be obtained by

$$\nu_i=\frac{c\operatorname{Re}\left(k_{0_i}\right)}{2\pi}. \tag{23}$$

The fact that the solutions of (22) are all found to be complex, even though the material losses have been neglected, shows that all resonant modes of isolated resonators are "leaky." The intrinsic quality factors Q_i of the ith modes due to radiation loss can therefore be defined as (details can be found, e.g., in [3] and [29])

$$Q_i=\frac{\text{stored energy}}{\text{radiated energy per cycle}}=\left|\frac{\operatorname{Re}\left(k_{0_i}\right)}{2\operatorname{Im}\left(k_{0_i}\right)}\right|. \tag{24}$$

The explicit form of the Q matrices depends also on the expansion functions, i.e., on the choices (9)–(11) (e.g., the regular spherical waves can also be used in (11) instead of the spherical harmonic, cf. [14]). However, the zeros of (22) should be independent of these choices and this fact can be used as a check on the numerical results. Once a search in the complex k_0 plane has yielded a Q matrix which satisfies (22) to a sufficient degree of accuracy, it is relatively easy to calculate a corresponding coefficient vector $\vec{\alpha}^{(N)}$ of the surface current on S_{N-1}, by, e.g., a Gaussian elimination procedure, provided the k_{0_i} is a simple zero of the Q matrix. In consequence, a normalized resonant field in the exterior region can be obtained by introducing the coefficient vector $\vec{\alpha}^{(N)}$ into (20) and then (2). The procedure for computing surface currents and resonant fields mentioned above is very similar to that used in the moment method [10]. However, we do not discuss the procedure in detail in the present paper.

III. Classification of Modes

In practical calculations the determinant in (22) can only be obtained from a truncated Q matrix. Therefore, only an approximation of the resonance frequency and quality factor of a certain mode can be obtained, except for concentric layered spherical objects of which the Q matrices are diagonal. As the truncation size, denoted by $l_{\max}$, increases, this approximation can be expected to converge to a definite value. Therefore the behavior of the results as a function of truncation order plays an important role in assessing the accuracy of the computed results.

For a Q matrix of truncation size $l_{\max}$ $(l=1,2,\cdots,l_{\max}$, and $m=0,1,\cdots,l$, cf. (3)), the matrix order is given by $2(l_{\max}+2)\times l_{\max}$. That means we have to calculate, for, e.g., $l_{\max}=10$, Q matrices of order 240×240 and their determinants in the search process. In the case of resonators with general geometry, most of the Q matrix elements computed from the surface integrations according to (15) do not vanish. However, for certain special geometries, such as axisymmetric bodies, the computations can be reduced substantially. In an axisymmetric case, the surface integrations in (15) degenerate to line integrations over the contours of corresponding surfaces, and all elements in off-diagonal blocks (where $m\neq m'$) are equal zero. A general form of the Q matrices for an axisymmetric object is written as follows:

$$
\boldsymbol{Q}=\left(\begin{array}{cccc|cccc|cccc|c}
\boldsymbol{A}^0_{ll'} & \mathbf{0} & \mathbf{0} & \mathbf{0} & & & & & & & & & \\
\mathbf{0} & \boldsymbol{D}^0_{ll'} & \mathbf{0} & \mathbf{0} & & \mathbf{0} & & & & \mathbf{0} & & & \mathbf{0}\\
\mathbf{0} & \mathbf{0} & \boldsymbol{A}^0_{ll'} & \mathbf{0} & & & & & & & & & \\
\mathbf{0} & \mathbf{0} & \mathbf{0} & \boldsymbol{D}^0_{ll'} & & & & & & & & & \\
\hline
 & & & & \boldsymbol{A}^1_{ll'} & \boldsymbol{B}^1_{ll'} & \mathbf{0} & \mathbf{0} & & & & & \\
 & \mathbf{0} & & & \boldsymbol{C}^1_{ll'} & \boldsymbol{D}^1_{ll'} & \mathbf{0} & \mathbf{0} & & \mathbf{0} & & & \mathbf{0}\\
 & & & & \mathbf{0} & \mathbf{0} & \boldsymbol{A}^1_{ll'} & -\boldsymbol{B}^1_{ll'} & & & & & \\
 & & & & \mathbf{0} & \mathbf{0} & -\boldsymbol{C}^1_{ll'} & \boldsymbol{D}^1_{ll'} & & & & & \\
\hline
 & & & & & & & & \boldsymbol{A}^2_{ll'} & \boldsymbol{B}^2_{ll'} & \mathbf{0} & \mathbf{0} & \\
 & \mathbf{0} & & & & \mathbf{0} & & & \boldsymbol{C}^2_{ll'} & \boldsymbol{D}^2_{ll'} & \mathbf{0} & \mathbf{0} & \mathbf{0}\\
 & & & & & & & & \mathbf{0} & \mathbf{0} & \boldsymbol{A}^2_{ll'} & -\boldsymbol{B}^2_{ll'} & \\
 & & & & & & & & \mathbf{0} & \mathbf{0} & -\boldsymbol{C}^2_{ll'} & \boldsymbol{D}^2_{ll'} & \\
\hline
 & \mathbf{0} & & & & \mathbf{0} & & & & \mathbf{0} & & &
\end{array}\right)
\begin{array}{ll}
\sigma\tau & \\
1e & \\ 2o & m=0 \\ 1o & \\ 2e & \\
1e & \\ 2o & m=1 \\ 1o & \\ 2e & \\
1e & \\ 2o & m=2 \\ 1o & \\ 2e & \\
\cdots &
\end{array}
$$

$$
\begin{array}{c|cccc|cccc|cccc|c}
\sigma'\tau'= & 1e & 2o & 1o & 2e & 1e & 2o & 1o & 2e & 1e & 2o & 1o & 2e & \cdots\\
 & & m'=0 & & & & m'=1 & & & & m'=2 & & &
\end{array}
$$

The decomposition of the Q matrices into smaller diagonal blocks indicates that we may search zeros for a particular value of the index m, which amounts to choosing a particular azimuthal dependence of the resonant field in advance. Furthermore, since the determinants of

$$\begin{pmatrix} A, & B \\ C, & D \end{pmatrix} \quad \text{and} \quad \begin{pmatrix} A, & -B \\ -C, & D \end{pmatrix}$$

are identical, the zeros need only be searched for in a block of order $2 \times l_{\max}$ for a fixed m ($m > 0$), which correspond to hybrid electromagnetic modes (HEM). For $m = 0$, the block is decoupled into even smaller pieces with respect to the two types of vector spherical waves $\vec{\psi}_{1e0l}$ and $\vec{\psi}_{2e0l}$. Since $\vec{\psi}_{1e0l}$ has only an $\hat{e}_\phi$ component while $\vec{\psi}_{2e0l}$ has only $\hat{e}_r$ and $\hat{e}_\theta$ components (cf. (3)), the zeros computed from the small block $A^0_{ll'}$ correspond to TE and from the block $D^0_{ll'}$ to TM resonant modes, respectively.

The zeros of the matrix determinant of the blocks can be searched for in the complex plane by means of, e.g., Muller's method [30], or a similar iterative procedure which does not require a knowledge of the derivative of the function whose zeros are being sought. The iteration is terminated when the change between two consecutively computed k_0 values is less than some prescribed small value. As a rule, these procedures must be supplied with two starting points reasonably close to the resonance frequency of the mode of interest. These starting points can be obtained, say, by a preliminary analysis of the scattering cross sections σ_s [13] of the resonator in the resonance range by using (19), (20), and

$$\sigma_s = \frac{\pi}{k_0^2} \sum_n |f_n|^2 \tag{25}$$

under the illumination of two perpendicular plane waves (TE and TM incident waves, as shown in Fig. 2). The peaks in the curves of the scattering cross sections can also be used to identify the resonant modes, as was done by Barber *et al.* in [19] for homogeneous dielectric spheres. The classes of TE, TM, and HEM modes are easily distinguished from the curves of the scattering cross sections, since we never see the peaks of TM resonant modes from the curves of the TE incidence and vice versa. The resonance frequencies of different modes of axisymmetric bodies from the same class are distinguished by three subscripts in this paper, $\nu_i \equiv \nu_{ml\delta+p}$. The first index, m, always refers to the azimuthal dependence of the mode as either $\cos m\phi$ or $\sin m\phi$, while the second and the third index, l and $\delta + p$, refer to the numbers of field extrema within the resonator in the radial and axial directions, respectively, where δ, $0 < \delta < 1$, is used to denote fractional half-period field variations in the resonator along the symmetry axis [3].

As an example, consider a cylindrical dielectric resonator in free space which has been analyzed by many authors using different methods. The resonator material is $\epsilon_1 = 38$, its radius is $a = 5.25$ mm, and its length is $L = 4.6$ mm. First the scattering cross sections σ_s are computed and then plotted in Fig. 2. The first peak on the left side of Fig. 2(a) can be identified as the $TE_{01\delta}$ mode because there

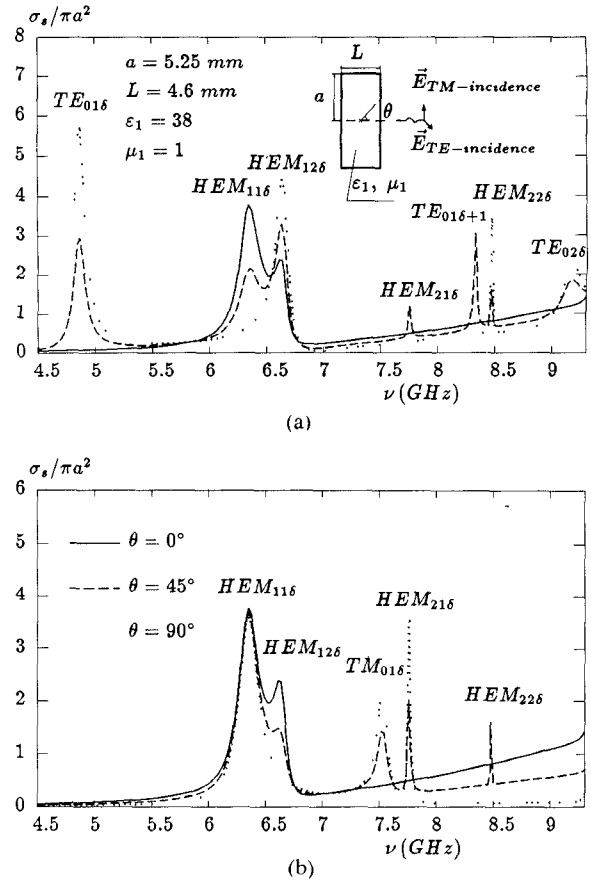

Fig. 2. Normalized scattering cross sections of a finite dielectric cylinder. (a) TE incidence. (b) TM incidence.

is no peak at the same position in Fig. 2(b) and a coupling between the incident field and the resonance can occur at all θ angles except normal incidences (e.g., $\theta = 0°$), whereas from neither $\theta = 0°$ nor $\theta = 90°$ can resonance be observed for the $TE_{01\delta+1}$ mode. The second peak from the left in Fig. 2(a) is identified as the $HEM_{11\delta}$, since the electric far field of the $HEM_{11\delta}$ modes does not have an $\hat{e}_\phi$ component (cf., e.g., [10]), and thus there is no peak response for the TE incidence from $\theta = 90°$ at this frequency. This fact suggests that the best experimental setup for measuring the resonance properties of the $TE_{01\delta}$ mode could be the worst for the $HEM_{11\delta}$ mode, i.e., accurate experimental observations of the resonance of the $HEM_{11\delta}$ mode are not possible for the resonator in free space, if one tries to observe a TE resonant field of the mode from $\theta = 90°$. Furthermore, the third peak in Fig. 2(a) is the $HEM_{12\delta}$ since no peak response for the TM incidence can be seen from $\theta = 90°$, and the fourth is the $HEM_{21\delta}$ because no peak is observed for the TE incidence from $\theta = 0°$, 90° or TM incidence from $\theta = 0°$. The remaining peaks could be classified in a similar way (cf. the field patterns of the resonant modes in, e.g., [10]). Of course, there exist many modes which have similar scattering characteristics as a function of θ at different frequencies, such as the $TE_{01\delta}$ and $TE_{02\delta}$ modes in Fig. 2. In these cases, a classification of these resonant modes requires calculations of the resonant field in the vicinity of the resonator.

TABLE I
COMPUTED RESONANCE FREQUENCIES AND QUALITY FACTORS VERSUS DIFFERENT TRUNCATION SIZES l_{max} COMPARED WITH MEASUREMENTS AS WELL AS WITH RESULTS FROM OTHER METHODS FOR A DIELECTRIC PILLBOX ($\epsilon_1 = 38$, $\mu_1 = 1$, $a = 5.25$ mm, $L = 4.6$ mm) IN FREE SPACE

Resonant Frequencies (GHz)								
l_{max}	$TE_{01\delta}$	$HEM_{11\delta}$	$HEM_{12\delta}$	$TM_{01\delta}$	$HEM_{21\delta}$	$TE_{01\delta+1}$	$HEM_{22\delta}$	$TE_{02\delta}$
6	4.8619	6.3391	6.6639	7.4659	7.7543	8.3127	8.5035	9.1722
8	4.8604	6.3450	6.6598	7.5371	7.7636	8.3336	8.4832	9.1470
10	4.8603	6.3450	6.6537	7.5370	7.7606	8.3315	8.4771	9.1521
12	4.8604	6.3450	6.6530	7.5373	7.7616	8.3308	8.4780	9.1535
14	4.8604	6.3450	6.6527	7.5380	7.7621	8.3310	8.4779	9.1337
16	4.8604	6.3450	6.6520	7.5384	7.7621	8.3311	8.4768	9.1535
Measured[10]	4.85	—	6.64	7.60	7.81	—	—	—
Moment Method[10]	4.829	6.333	6.638	7.524	7.752	—	—	—
Perturbation of PMC[3]	4.8551	—	—	—	—	8.1937	—	—
Asymptotic Method[8]	4.87	—	—	—	—	—	—	—
Quality Factors due to radiation								
l_{max}	$TE_{01\delta}$	$HEM_{11\delta}$	$HEM_{12\delta}$	$TM_{01\delta}$	$HEM_{21\delta}$	$TE_{01\delta+1}$	$HEM_{22\delta}$	$TE_{02\delta}$
6	40.848	30.853	57.009	59.199	333.28	303.43	1206.0	45.804
8	40.819	30.945	54.059	75.042	337.51	301.42	1137.9	44 065
10	40.819	30.896	51.082	75.790	339.08	300.97	1038.6	43.645
12	40.820	30.852	50.809	76.075	337.98	300.91	1036.5	43.743
14	40.819	30.849	50.705	76.694	337.55	301.00	1030.0	43.747
16	40.819	30.853	50.316	76.921	337.66	301.02	1018.4	43 736
Measured[10]	51	—	64	86	204	—	—	—
Moment Method[10]	45.8	30.7	52.1	76.8	327.1	—	—	—
Asymptotic Method[8]	42.31	—	—	—	—	—	—	—

The method of extracting the starting points from the peaks of the cross sections is very similar to that of analyzing experimental curves in transmission measurement, i.e., taking the position of a peak as an approximate resonance frequency and the ratio of the height to the half width of the peak as an approximate quality factor. From these starting points, more accurate resonance frequencies and Q factors are computed and listed in Table I. The convergence of the present method is also shown in Table I for different truncation orders. The agreement between the results of the null-field method and other methods is reasonably good.

The null-field method has also been used to compute a universal mode chart for cylindrical dielectric resonators with $\epsilon = 38$ in free space. The chart is shown in Fig. 3, displaying the value of $k_0 a$ and the quality factor as a function of the ratio, a/L, of the resonator radius to length for the eight lower modes listed in Table I. Five of the $k_0 a$ curves are also compared with the results computed using the method of moments [9] in Fig. 3. In general the results from the two methods agree very well except for those of the $TM_{01\delta}$ mode at higher aspect ratio (i.e., at the two ends of the $TM_{01\delta}$ curve). Moreover, curves computed using the present method are very smooth and no kinks can be observed on the present scale. Some computed results for the $TE_{01\delta}$ and $HEM_{11\delta}$ modes from a general mode-matching method [12] are also included in Fig. 3(a) for comparison. A good agreement can be observed. From Fig. 3(b) we see that the $HEM_{11\delta}$ mode has the lowest Q value, i.e., the strongest radiation effect, when $a/L > 0.85$. This mode has been utilized in designing a resonant cylindrical dielectric cavity antenna [31]. However, when the length, L, is equal to or greater than the diameter, $2a$, of a pillbox (for the case $\epsilon = 38$), the $TM_{01\delta}$ mode seems more suitable for use in an antenna.

As a third example, we show how the resonance frequencies and quality factors change when the above-mentioned cylindrical homogeneous resonator gradually changes half of its lateral wall and upper flat surface into half a spheroidal surface (cf. Fig. 4) according to the superellipsoid function $(x^n/a^n + y^n/b^n = 1$, with n changing from infinity to 2). Fig. 4 depicts the theoretical mode chart of some lower resonant modes of such a resonator. From this figure one finds that, as expected, neither resonance frequencies nor Q factors vary very much when the upper edge of the pillbox is rounded off (the lower flat surface of the pillbox is supposed to be mounted on a substrate with its electrical properties close to those of free space) and that curves of different modes do not intersect each other; i.e., no degeneration occurs during smoothening.

In this section, the null-field method has been applied to a study of homogeneous dielectric resonators. Examples of composite resonators are given in the next section.

IV. COMPOSITE RESONATORS

Most composite resonators are designed with the purpose of obtaining frequency tunable resonant elements in microwave components, such as microwave filters and oscillators [32]. Taking several composite structures of resonators as examples, we compute frequency charts using the null-field method in this section.

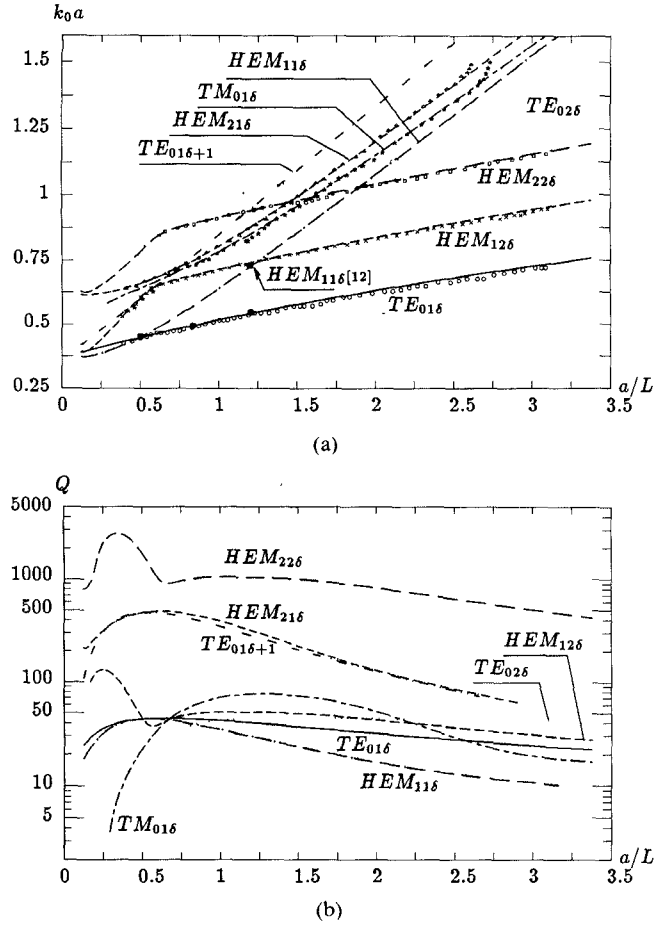

Fig. 3. Universal mode chart for isolated cylindrical dielectric resonators with relative permittivity $\epsilon_1 = 38$. Lines are computed using the present method. The bullets • • • are from the mode matching method in [12]. Other markers are from the method of moment [9]. (a) Resonance. (b) Quality factors.

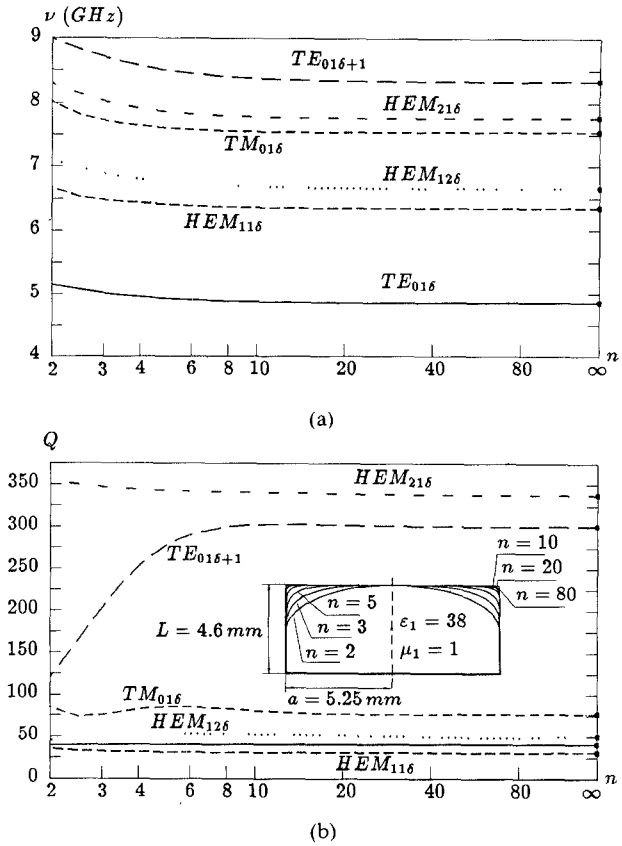

Fig. 4. Resonance frequencies and quality factors of the six lowest modes of a partially smoothened cylinder versus the exponential, n, of the superellipsoid function $(x^n/a^n + y^n/b^n = 1)$. The values indicated by bullets, • • •, on the right-hand side vertical axes are extracted from the corresponding curves in Fig. 3 for a pillbox resonator with the same radius and length. (a) Resonance frequencies. (b) Quality factors.

We first consider a structure of two dielectric (or ferrite) disks which can be used in either a filter [33] or a circulator [34]. The individual resonators in the structure are cylindrical disks of radius r and thickness t which are mounted coaxially and separated by a distance d. Assuming that each resonator has the same electric constant and that they are identical in size, the whole structure can be described by taking S_0 as the surface of a pillbox with radius r and length $L = 2t + d$ filled with the material of the disks, and the core, V_2, as a shallower pillbox with the same radius r and length d having electromagnetic properties the same as the exterior medium (cf. Fig. 5). The resonance frequencies of the two lowest TE modes, $TE_{01\delta}$ and $TE_{01\delta+1}$, as functions of the distance d between the two disks are computed and plotted in Fig. 5 for a double-disk structure used in a frequency-stabilized band-rejection filter. Some measured results [33] are also included in Fig. 5 for comparison. The maximum relative difference of calculated results with respect to measurements is 1.85 percent for the case $\epsilon = 96$ and 2.90 percent for $\epsilon = 80$, respectively. The frequency tuning range for d varying from 0 to t is about 15 percent for both cases. In this range, the relation between frequency and k is relatively far from linear. If d is sufficiently large, the resonance frequencies of both the $TE_{01\delta}$ and $TE_{01\delta+1}$ modes of the double disk gradually approach those of the $TE_{01\delta}$ mode of one of the single disks.

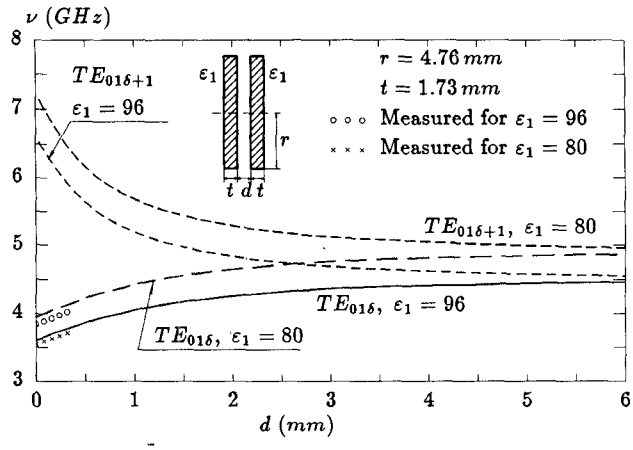

Fig. 5. Resonance frequencies of the two lowest TE modes of a double dielectric disk resonator with different permittivities versus the distance between the two disks. The measured results are adopted from [33].

The double-disk resonator is a kind of mechanical frequency tuning device. The resonance frequency can also be tuned electrically by attaching a microwave ferrite disk on

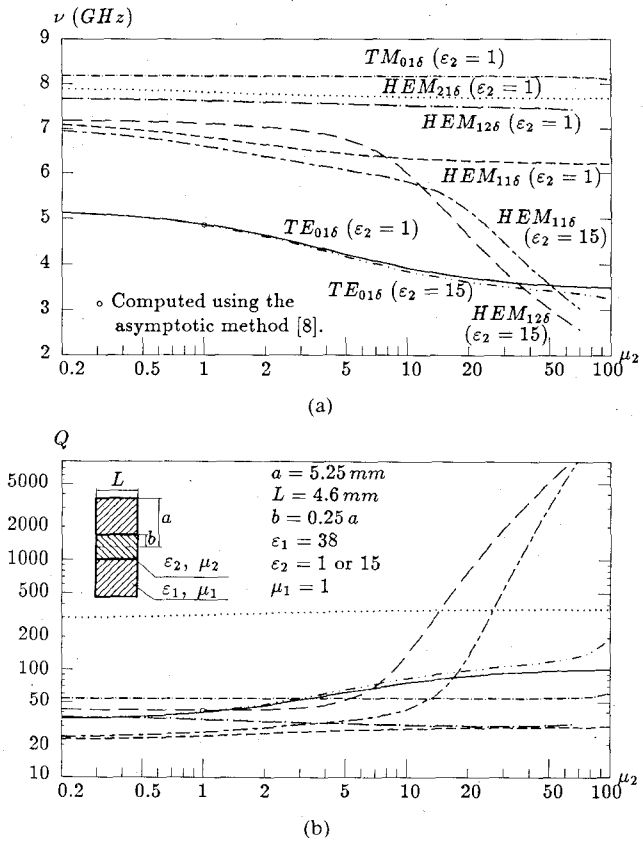

Fig. 6. Resonance frequencies and quality factors of seven lower modes of a dielectric ring with a ferrite cylindric plug versus the permeability of the plug. The circles in the figure represent calculations using the asymptotic method for the dielectric ring ($\epsilon_2 = 1$, $\mu_2 = 1$). (a) Resonance frequencies. (b) Quality factors.

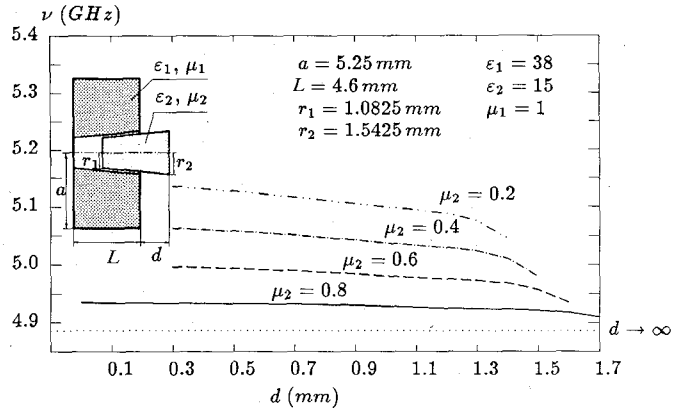

Fig. 7. Resonance frequencies of the $TE_{01\delta}$ mode of a conically shaped dielectric ring with a ferrite conical plug versus the position of the plug for different permeabilities.

a pillbox resonator and applying a magnetic field to it (cf., e.g., [35]). The magnetic field controls the magnetic properties of the ferrite, resulting in a shift in the resonance frequency (the lowest mode $TE_{01\delta}$ was used). Tuning bandwidths of the order of 3 percent for this construction have been reported [35]. Since the magnetic field is strongest down the center, instead of on the flat faces, of a cylindrical resonator for the $TE_{01\delta}$ mode, one would expect to achieve a wider frequency tuning range by removing a cylindrical dielectric plug from the resonator center and inserting a ferrite one. Assuming that the permeability tensor of the ferrite can be expressed by a scalar (e.g., a demagnetized polycrystalline ferrite material, cf. [34]), and noting that the permeability of partially magnetized ferrites is a certain function of the strength of the applied magnetic field [36], one can approximately describe the characteristic of a ferrite under an applied tunable magnetic field by changing the permeability of the ferrite. In Fig. 6, a chart of resonance frequencies and Q values versus different permeability values of a ferrite plug mounted in a dielectric ring is given. The ring has the same radius a, length L, and permittivity ϵ_1 as the pillbox resonator in the first example in Section III. From Fig. 6, one observes that the permittivity of the plug could be changed from $\epsilon_2 = 1$ to 15 without disturbing the resonant frequency of the $TE_{01\delta}$ mode too much since the electric field is weak for that mode near the resonator center. One also observes that the $HEM_{12\delta}$ mode, when $\epsilon_2 = 15$ and $\mu_2 > 38$ in the plug, becomes the lowest mode with a very high Q value, which suggests that a much smaller resonator can be designed using this mode without any metallic housing, provided a material with very high permeability and very low loss is available. Furthermore, the frequency tuning range can be easily obtained from Fig. 6 if one knows the relation between the permeability of a ferrite and the strength of the applied magnetic field.

In order to increase the tuning range, a combination of mechanical and electrical tuning may be employed by giving the hole of the dielectric ring as well as the ferrite plug a conical shape, as shown in Fig. 7. However, from the calculated results in this figure, one can see that the resonance frequency of the $TE_{01\delta}$ mode is not very sensitive to displacements of the ferrite plug so long as the permeability of the plug remains close to unity.

V. Conclusion

In this article we have employed an approach within the general framework of the null-field method to investigate the resonance properties of several kinds of composite resonators. For the composite rotationally symmetric resonators discussed in the present paper, the null-field method shows good convergence and reasonable agreement with other computed and measured results. We are also aware in our numerical experiments that for certain geometries, e.g., a pillbox attached to a ferrite cylindrical disk on one flat face, the expansion functions chosen in (11) do not yield convergent results as good as those produced by the regular spherical vector wave function (cf., e.g., [14]). This fact suggests, as is mentioned in Section II, that alternative choices of expansion functions are often helpful in checking the computed results. All computed results for composite resonators reported in the present paper have been checked by using at least two different expansions.

Finally, we note that it is of interest to carry out a corresponding investigation concerning metallic shielded

composite resonators. The results from such an investigation will be reported in a subsequent paper.

ACKNOWLEDGMENT

The author is indebted to Prof. S. Ström and Dr. G. Kristensson for their valuable advice and helpful comments.

REFERENCES

[1] S. B. Cohn, "Microwave bandpass filters containing high-Q dielectric resonators," *IEEE Trans. Microwave Theory Tech.*, vol. MTT-16, pp. 218–227, Apr. 1968.

[2] T. Itoh and R. Rudokas, "New method for computing the resonant frequencies of dielectric resonator," *IEEE Trans. Microwave Theory Tech.*, vol. MTT-25, pp. 52–54, Jan. 1977.

[3] D. Kajfez and P. Guillon Eds., *Dielectric Resonators*. Norwood, MA: Artech House, 1986.

[4] K. A. Zaki and C. Chen, "New results in dielectric-loaded resonators," *IEEE Trans. Microwave Theory Tech.*, vol. MTT-34, pp. 815–824, July, 1986.

[5] S. Maj and M. Pospieszalski, "A composite, multilayered cylindric resonator," in *1984 IEEE MTT-S Int. Microwave Symp. Dig.*, pp. 190–192.

[6] J. Krupka, "Computations of frequencies and intrinsic Q factors of TE_{0nm} modes of dielectric resonators," *IEEE Trans. Microwave Theory Tech.*, vol. MTT-33, pp. 274–277, Mar. 1985.

[7] M. Verplanken and J. Van Bladel, "The electric-dipole resonances of ring resonators of very high permittivity," *IEEE Trans. Microwave Theory Tech.*, vol. MTT-27, pp. 328–333, Apr. 1979.

[8] R. DeSmedt, "Correction due to a finite permittivity for a ring resonator in free space," *IEEE Trans. Microwave Theory Tech.*, vol. MTT-32, pp. 1288–1293, Oct. 1984.

[9] A. W. Glisson, D. Kajfez, and J. James, "Evaluation of modes in dielectric resonators using a surface integral equation formulation," *IEEE Trans. Microwave Theory Tech.*, vol. MTT-31, pp. 1023–1029, Dec. 1983.

[10] D. Kajfez, A. W. Glisson, and J. James, "Computed modal field distributions for isolated dielectric resonators," *IEEE Trans. Microwave Theory Tech.*, vol. MTT-32, pp. 1609–1616, Dec. 1984.

[11] R. E. Collin and D. A. Ksienski, "Boundary element method for dielectric resonators and waveguides," *Radio Sci.*, vol. 22, no. 7, pp. 1155–1167, Dec. 1987.

[12] M. Tsuji, H. Shigesawa, and K. Takiyama, "Analytical and experimental investigations on several resonant modes in open dielectric resonators," *IEEE Trans. Microwave Theory Tech.*, vol. MTT-32, pp. 628–633, June 1984.

[13] P. C. Waterman, "Symmetry, unitarity, and geometry in electromagnetic scattering," *Phys. Rev. D*, vol. 3, no. 4, pp. 825–839, 1971.

[14] S. Ström and W. Zheng, "Basic features of the null field method for dielectric scatterers," *Radio Sci.*, vol. 22, no. 7, pp. 1273–1281, Dec. 1987.

[15] S. Ström and W. Zheng, "The null field approach to electromagnetic scattering from composite objects," *IEEE Trans. Antennas Propagat.*, vol. 36, pp. 376–382, Mar. 1988.

[16] W. Zheng, "The null field approach to electromagnetic scattering from composite objects: The case with three or more constituents," *IEEE Trans. Antennas Propagat.*, vol. 36, pp. 1396–1400, Oct. 1988.

[17] A. Boström, "Passbands and stopbands for an electromagnetic waveguide with a periodically varying cross section," *IEEE Trans. Microwave Theory Tech.*, vol. MTT-31, pp. 752–756, Sept. 1983.

[18] L. Lundqvist, "A penetrable dielectric waveguide with periodically varying circular cross section," *IEEE Trans. Microwave Theory Tech.*, vol. MTT-35, pp. 282–287, Mar. 1987.

[19] P. W. Barber, J. F. Owen, and R. K. Chang, "Resonant scattering for characterization of axisymmetric dielectric objects," *IEEE Trans. Antennas Propagat.*, vol. AP-30, pp. 168–172, Mar. 1982.

[20] G. Kristensson, "Natural frequencies of circular disks," *IEEE Trans. Antennas Propagat.*, vol. AP-32, pp. 442–448, May 1984.

[21] A. Boström, "Time-dependent scattering by a bounded obstacle in three dimensions," *J. Math. Phys.*, vol. 23, no. 6, pp. 1444–1450, 1982.

[22] A. Boström, "Time-dependent electromagnetic scattering by a bounded obstacle in three dimensions," in *Proc. Int. Workshop Mathematics on Classical Scattering*, (Glasgow), Aug. 1983.

[23] P. J. Moser and H. Überall, "Complex eigenfrequencies of axisymmetric perfectly conducting bodies," *Proc. IEEE*, vol. 71, pp. 171–172, 1983.

[24] W. E. Howell and H. Überall, "Complex frequency poles of radar scattering from coated conducting spheres," *IEEE Trans. Antennas Propagat.*, vol. AP-32, pp. 624–627, June 1984.

[25] W. Zheng, "The complex resonant frequencies of open composite dielectric resonators," in *Proc. 17th European Microwave Conf.* (Rome, Italy), vol. 2, Sept. 1987, pp. 945–950.

[26] W. Zheng and S. Ström, "The null field approach to scattering from composite objects: The case of concavo-convex constituents," *IEEE Trans. Antennas Propagat.*, vol. 37, Mar. 1989.

[27] B. Peterson and S. Ström, "T-matrix formulation of electromagnetic scattering from multilayered scatterers," *Phys. Rev. D*, vol. 10, pp. 2670–2684, 1974.

[28] D. S. Wang and P. W. Barber, "Scattering by inhomogeneous nonspherical objects," *Appl. Opt.*, vol. 18, no. 8, pp. 1190–1197, 1979.

[29] A. Julien and P. Guillon, "Electromagnetic analysis of spherical dielectric shielded resonators," *IEEE Trans. Microwave Theory Tech.*, vol. MTT-34, pp. 723–729, 1986.

[30] S. D. Conte and C. De Boor, "Elementary Numerical Analysis. *New York: McGraw-Hill*, 1980.

[31] S. A. Long, M. McAllister, and L. C. Shen, "The resonant cylindrical dielectric cavity antenna," *IEEE Trans. Antennas Propagat.*, vol. AP-31, pp. 406–412, May 1983.

[32] J. K. Plourde and C. L. Ren, "Application of dielectric resonators in microwave components," *IEEE Trans. Microwave Theory Tech.*, vol. MTT-29, pp. 754–770, Aug. 1981.

[33] M. A. Gerdine, "A frequency-stabilized microwave bend-rejection filter using high dielectric constant resonators," *IEEE Trans. Microwave Theory Tech.*, vol. MTT-17, pp. 354–359, July 1969.

[34] J. Helszajn and J. Sharp, "Dielectric and permeability effects in HE_{111} open demagnetized ferrite resonators," *Proc. Inst. Elec. Eng.*, vol. 133, pt. H, no. 4, pp. 271–276, Aug. 1986.

[35] A. N. Farr, G. N. Blackey, and D. Williams, "Novel technique for electronic tuning of dielectric resonator," in *Proc. 13th European Microwave Conf.* (Nürnberg, Germany), 1983, pp. 791–796.

[36] J. J. Green and F. Sandy, "Microwave characterization of partially magnetized ferrites," *IEEE Trans. Microwave Theory Tech.*, vol. MTT-22, pp. 641–645, June 1974.

Wenxin Zheng was born in Beijing, China, in 1953. He received the M.S. degree in electrical engineering from the graduate school of the North China Institute of Electric Power in 1982. He is currently pursuing the Ph.D. degree in the Department of Electromagnetic Theory at the Royal Institute of Technology in Stockholm, Sweden.

Since 1984 he has held the position of Lecturer in the graduate school of the North China Institute of Electric Power. His primary field of interest concerns computer solutions of electromagnetic field analysis problems. He has done research on applying finite element and finite difference methods in guided wave problems. He is currently engaged in the application of numerical methods to direct and inverse scattering and resonance problems for composite objects.